People Identification Using Floor Pressure Sensing and Analysis

Gang Qian, *Member, IEEE*, Jiqing Zhang, and Assegid Kidané, *Member, IEEE*

***Abstract*—This paper presents an approach to people identification based on gait using floor pressure data. By using a large-area, high-resolution pressure sensing floor, we are able to obtain both the 1D pressure profile and 2D position trajectories of the centers of pressure (COP) of both feet to form a 3D COP trajectories over a footstep. From the 3D COP trajectories of a pair of footsteps, a set of features are extracted and used together with other features such as the mean pressure and stride length for people identification. The Fisher linear discriminant is used as the classifier. The speed-invariant properties of different features are examined and we have shown that the pressure features have good speed-invariance properties, much better than the stride length feature. The proposed algorithm has been extensively tested using a floor pressure dataset collected from 11 subjects in different walking styles, including varying speed walking and free style walking. Decent people identification results have been obtained using the proposed method with an average recognition rate of 92.3% and false alarm rate of 6.79% using the best performing feature set.**

***Index Terms*—Biometrics, gait recognition, pressure analysis.**

I. Introduction

RECOGNIZING people based on gait is an important area in biometrics with applications in homeland security, access control, and human computer interaction. While most research for people identification using gait has been focused on computer vision based techniques, there has been research addressing gait recognition using foot pressure information [1], [4]–[6], [8]–[12], [16]–[18], and [21]. For example, Orr and Abowd [8] have researched people identification based on the pressure profile over time during a foot step on a load-cell sensor. The footstep profile features used in such approaches include the mean, the standard deviation, and the duration of the pressure profile, the overall area under the profile, and pressure value and the corresponding time of some key points such as the maximum point in the first and last halves of the profile and the minimum point between them. In these approaches, due to the nature of load-cell-based pressure sensing, the spatial pressure distribution during a foot step is not measured and only the amount of pressure and the corresponding time can be used for feature extraction and people identification. Therefore, the load-cell-based gait identification approaches do not take into account the spatial pressure distribution and features such as the trajectories of center of pressure (COP). On the other hand, Jung *et al.* [5], [6] used a mat-type pressure sensor for gait recognition based only on the 2D COP trajectory. To recognize a person based on the foot pressure measured during a gait cycle, it is important to extract both spatial features such as the trajectories of COP and footstep pressure profile features. To address this issue, in this paper we present a gait-based people identification method using foot pressure obtained using a pressure sensing floor. Our goal is to develop a system that can reliably identify a group of 5–20 people. By using a large-area, high-resolution pressure sensing floor, we were able to extract features from both the trajectories of the COP and the pressure profile of left and right foot steps during a gait cycle. In our proposed approach, the Fisher linear discriminant has been used as the classifier for people recognition from pressure features. Encouraging results have been obtained using the proposed method with an average recognition rate of 91% and false alarm rate of 8% using pairwise footstep data from 11 subjects. Experimental results show that the proposed method led to better or comparable results compared to existing methods. In the study reported in this paper, to ensure the quality of the pressure data and extracted COP trajectories, we only focused on the case in which the subjects walk on the pressure sensing floor with their shoes off. In our future work, we will study the shod case, which is a more realistic scenario in many applications.

This paper is an extended version of our previous conference paper [16], in which we present a similar people identification framework using floor pressure sensing and analysis. The results reported in [16] are limited in a few aspects. For example, data used in [16] was collected in only one scenario with walking in a straight line at normal speed. It was not clear how the proposed algorithm can work in varying walking speeds and directions. To further evaluate the proposed algorithm, additional data sets have been collected in more complicated scenarios with changing walking speed and direction. Results based on the enhanced data set are reported in this paper.

The organization of this paper is as follows. An overview of the pressure sensing floor used for people identification is given in Section II. In Section III, key preprocessing steps are presented, including clustering and tracking of footprints using mean-shift, recognition of the left and right feet, and rectification of COP trajectories. Sections IV and V are focused on

Manuscript received December 15, 2009; revised February 04, 2010; accepted February 18, 2010. Date of current version July 14, 2010. This work was supported in part by the U.S. National Science Foundation on CISE-RI 0403428 and IGERT 0504647. Any opinions, findings and conclusions or recommendations expressed in this material are those of the authors and do not necessarily reflect the views of the U.S. National Science Foundation (NSF). The associate editor coordinating the review of this paper and approving it for publication was Prof. Ralph Etienne-Cummings.

The authors are with the School of Arts, Media and Engineering, Arizona State University, Tempe, AZ 85287 USA (e-mail: gang.qian@asu.edu; jiqing.zhang@asu.edu; assegid.kidane@asu.edu).

Color versions of one or more of the figures in this paper are available online at http://ieeexplore.ieee.org.

Digital Object Identifier 10.1109/JSEN.2010.2045158

feature extraction from COP trajectories and people identification using these features in a Fisher discriminant analysis framework, respectively. Experimental results and performance analysis are presented in Section VI. We finally conclude this paper and present future work in Section VII.

II. An Overview of the Pressure Sensing Floor

The pressure sensing floor system [14], [15] we use for people recognition features a modularized design and it consists of 96 networked pressure sensing mat modules. Each mat module contains a pressure sensing mat (Tekscan 5315) to measure the applied pressure, and peripheral elements such as a microcontroller, an Ethernet controller, and customized supporting circuitry for data collection and communication. These pressure sensing mat modules are arranged in a rectangular (12×8) shape spanning a total sensing area of 221 ($17' \times 13'$) square feet. Each pressure sensing mat has a 48×42 (2016) grid of force sensing resistor (FSR)-based pressure sensors in a 48.8 cm $\times$ 42.7 cm active area, leading to a resolution of six sensors per square inch. The entire pressure sensing floor system has a scanning rate up to 44 Hz with a latency of 25 ms. To allow for multimodal movement data collection, the pressure sensing floor is synchronized with marker-based motion capture system and video camera array through shared external clock. More details about the pressure sensing floor can be found in [15].

For a specific application, a customized pressure sensing floor can be built with the proper size and shape to fit the particular pressure sensing needs. To build a pressure sensing floor such as the one we used in our research can be expensive, depending on the size and the number of pressure sensing mat modules used in the system. In average, it will cost around $600 per sensing mat module to duplicate our pressure sensing floor system, including the mat itself and the peripheral supporting elements. Although our pressure sensing floor was costly to build, recent advances in pressure sensing have made high-quality, low-cost pressure sensing floor possible. For example, in [23] a novel pressure sensing principle called Interpolating Force Sensitive Resistance (IFSR) has been introduced and demonstrated for high-accuracy, high-resolution (87 dot per inch), and high-frame rate ($\sim$60 Hz) pressure sensing. Another feature of IFRS is its low cost [23]. The availability of such high-quality and low-cost pressure sensing techniques will make pressure sensing systems, including large-area pressure sensing floors, a lot more affordable to both researchers and consumers.

III. Preprocessing of Floor Data

To recognize people using gait based on floor pressure, it is necessary to first preprocess the raw pressure data obtained using the pressure sensing floor and then extract features that can be used for gait recognition. A number of tasks need to be accomplished by this preprocessing step, including pressure data clustering, tracking of the cluster centers, recognition of left and right feet, estimation of walking directions, and rectification of the COP trajectories.

A. Clustering and Tracking of Centers of Pressure Using Mean-Shift

In our research, the mean-shift algorithm [2], [20] is used to cluster floor pressure data and track the center of pressure over time. Mean-shift is an iterative shifting process to find the local modes of the density from a set of data points without actually estimating the density. Given the kernel function $G(\cdot)$, its window size h, and sample important weight $w(x)$, the mean-shift procedure starting from a data point x has the following steps.

1) Compute the mean-shift vector $M_h(x)$ starting from x

$$M_{\boldsymbol{h}}(x) = \frac{\sum_{i=\mathbf{1}}^{n} G\left(\frac{x_i - x}{\boldsymbol{h}}\right) w(x_i)(x_i - x)}{\sum_{i=\mathbf{1}}^{n} G\left(\frac{X_i - X}{\boldsymbol{h}}\right) w(x_i)}. \tag{1}$$

2) Find the weighted mean of the data points around x

$$x \leftarrow x + M_{\boldsymbol{h}}(x). \tag{2}$$

It is shown in [2] and [20] that starting from a data point x, iteratively updating the weighted mean following the mean-shift procedure using (1) and (2) leads to convergence to the local mode for proper selected kernels, e.g., Gaussian and truncated Gaussian kernels. In our case the data samples are the 2D locations of points on the floor with active pressure readings. In our experiments, the positions of pressure data points are first clustered through the blurring process [2] using a Gaussian kernel. In a blurring process, mean-shift procedures are carried out from all the data points. After one cycle of mean-shift iteration, all the data points will be replaced by their corresponding weighted means from (2) and then the next cycle of iteration will start based on the updated data points. Such iterative procedure introduces "successive blurring of the data set" [2]. The mean-shift procedures starting from different points in the data set will converge to the modes of the underlying density of the data samples. In our experiments, the observed pressure at a point is then used as the corresponding weight for this point. Once the process has converged, the data set will be tightly packed into clusters, with all of the data points located closely to the center of that cluster. The process is said to have converged either after the maximum number of iterations defined by the algorithm is reached or earlier when the mean shift of centers becomes less than the convergence threshold. After convergence, each cluster is assigned with a unique cluster ID number and every data point has a "label" associated with corresponding cluster. For every subsequent pressure data frame, centers from the previous frame are updated through the mean-shift algorithm (1) using current observed pressure values as weights and checked for convergence. In practice, entirely new data points resulting in new cluster centers can occur if there are groups of data points not assigned to any existing cluster centers. Fig. 1 shows clustering and tracking results of the pressure data over about 1.5 gait cycles. The red dots indicates the cluster centers and the white digits their ID numbers. During a *footstep*, which is defined as the period between the heel-strike and the toe-off of a foot, the COP of the foot can be correctly tracked using the mean-shift algorithm since the corresponding cluster ID is maintained. In addition, we define the *pressure related to a COP* as the sum of the pressure values of all the samples in the corresponding cluster. As a result, over a footstep, a 3D COP trajectory can be obtained, including 2D position trajectories of the COP and the pressure profile over time.

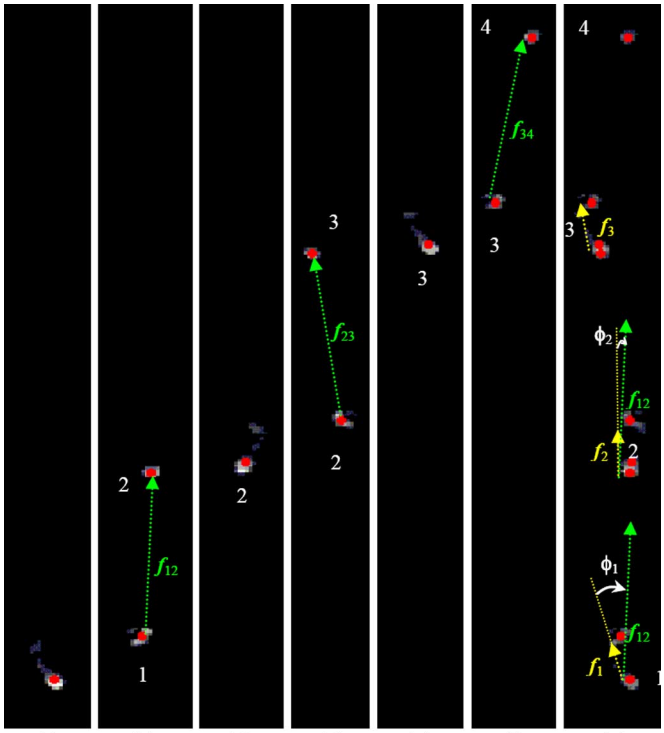

Fig. 1. Clustering and tracking results over about one and half gait cycles. Columns (a) through (f) show snap shots of observed floor data and corresponding COPs (red dots) and their ID numbers (white digits). It can be seen that the IDs of the COP remain unchanged during a single footstep. The inter-foot vectors are shown by the green arrows. Subfigure (g) shows overlapped floor data from (a) to (f) so that the intrafoot vectors can be visualized (the yellow arrows) properly.

B. Foot Recognition

It is important to separate the left and right feet so that proper features can be extracted for people identifications. In our research, we take a simple and efficient approach to foot recognition based on the COP trajectories obtained using the mean-shift algorithm. Let $C_1 = \{c_1(s_1), \ldots, c_1(e_1)\}$ and $C_2 = \{c_2(s_2), \ldots, c_2(e_2)\}$ be two successively detected and tracked COP trajectories over two adjacent footsteps, footstep 1 and footstep 2, where $c_1(s_1)$ and $c_1(e_1)$ represent the position of the heel-strike and toe-off of one foot, and $c_2(s_2)$ and $c_2(e_2)$ that of the other foot, and s and e are time indices. The goal is to identify which footstep corresponds to the left foot and which one to the right foot. To do that, we define two types of vectors: the intra-foot vectors and the inter-foot vectors. The intra-foot vectors are vectors from the heel-strike position to the toe-off position during a single footstep, for example, $\boldsymbol{f}_1 = (c_1(s_1) \rightarrow c_1(e_1))$ and $\boldsymbol{f}_2 = (c_2(s_2) \rightarrow c_2(e_2))$. The inter-foot vector is from the toe-off of the first footstep to the heel-strike of the second footstep. In this example, $\boldsymbol{f}_{12} = (c_1(e_1) \rightarrow c_2(s_2))$.

Let $\phi_1 = \angle \boldsymbol{f}_1 \boldsymbol{f}_{12}$, and $\phi_2 = \angle \boldsymbol{f}_2 \boldsymbol{f}_{12}$ be the clockwise acute angles (possibly negative) from the intra-foot vectors to the inter-foot vector. By using ϕ_1 and ϕ_2, it is easy to separate the left foot from the right foot since when footstep 1 is the left foot, $\phi_1 > \phi_2$ and *vice versa*. See Fig. 1 for an example.

The proposed foot recognition method is also robust to handle some special cases. For example, assume that a subject started walking with the step sequence left-right-left-right, and then after a short pause, the subject continued to walk with an altered step sequence, e.g., right-left-right-left. In this case, the second left-step in the first sequence will be paired up with the first right-step in the second sequence and their intra-foot vectors and the corresponding inter-foot vector will be used for foot recognition. The last right-step in the first sequence before the pause will simply be skipped. This is because when this footstep was finished with toe-off and the corresponding intra-foot vector became available, there was no matching intra-foot vector for the other foot. At this moment, the left foot was still supporting the body and its intra-foot vector was not available yet. For this reason, the last right-step in the first sequence will not be recognized. Instead, the first right-step in the second sequence will be recognized together with the second left-step in the first sequence. The short pause and the switching of the footstep order will not cause any confusion to the proposed foot recognition method.

C. Rectification of COP Trajectories

For each foot step, a 3D COP curve can be obtained as a function over time, which consists of the 2D position trajectories and the corresponding floor pressure trajectories. After the separation of the left and right feet, the 3D COP curves of both feet spanning over a gait cycle can be obtained. At this point, the 2D position trajectories are in a global floor-centered coordinate frame. To make the COP trajectories invariant to the walking direction of the person, a rectification step is needed to rotate the COP trajectories so that the resulting trajectories are represented in a local foot-centered coordinate frame. In our research, we first estimate the walking direction as the mean of the left and right intra-foot vectors over a single gait cycle. This walking direction is then used as the y axis direction of the local coordinate frame and the x axis direction is easily determined by the right-hand-rule so that the resulting z axis (also the pressure-axis) is up. The origin of the local foot-centered frame is taken as the heel-strike point of the corresponding footstep. Fig. 2 shows the mean plots of the COP and pressure trajectories of the left (a) and right (b) footsteps of 11 subjects. Panels (c) (d) and (e) (f) are the projected 2D position and 1D pressure trajectories. Figs. 3–5, respectively, show samples of the complete 3D COP and 2D position COP trajectories, and 1D pressure profiles of the left (left panels) and right footsteps from the seventh (first rows) and the tenth subjects. The seventh subject is 170 cm tall and weighs 83 kg and the tenth subject 183 cm and 75 kg. From these plots, it can be seen that there is certain inconsistency in the COP trajectories of the same subject from trial to trial. Meanwhile, similarity exists in the COP trajectories across subjects. Thus it is important to extract and select reliable features from the 3D COP trajectories to allow for robust people identification.

In these figures, 2D position COP trajectories are in **centimeters** (**cm**). The pressure readings are in **digital pressure values** (**dpv**) and 1 digital pressure value is equal to **0.521 pound per square inch** (**psi**). This mapping from digital pressure values to psi was determined through a floor pressure sensor calibration process. A person of 160 lbs and 1.8 m tall in anatomical neutral pose standing on the pressure sensing floor will result in an overall ground pressure of about 1800 dpv.

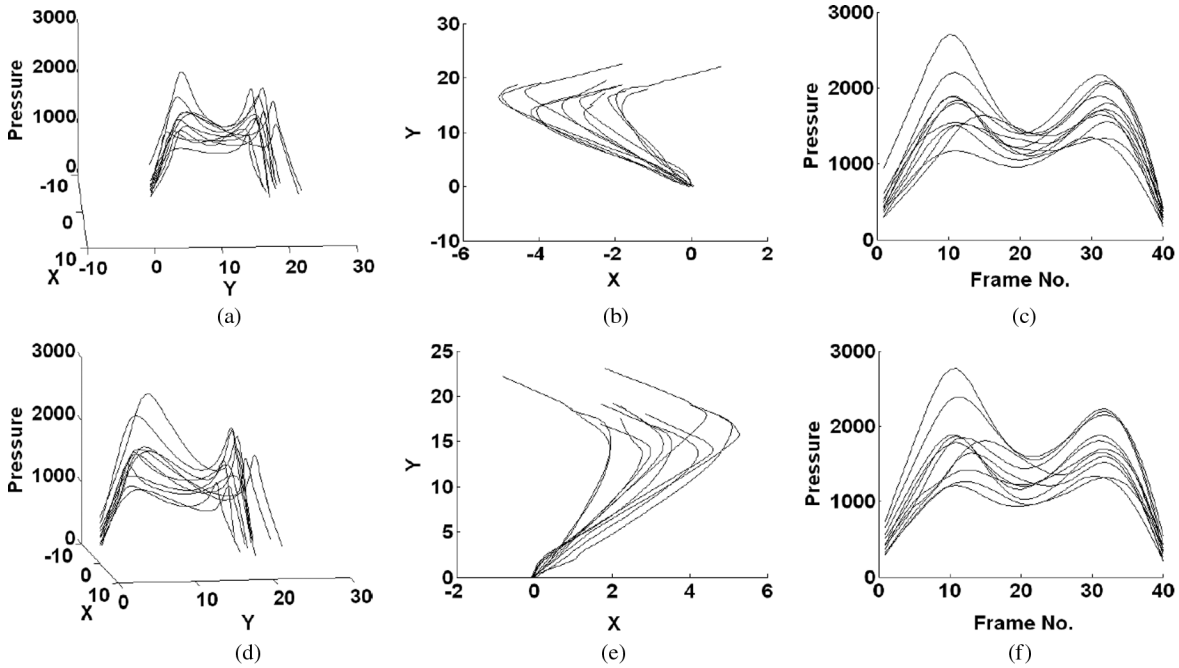

Fig. 2. Mean COP trajectories of the left (top panel) and right (bottom panel) footsteps using data from 11 subjects. (a) and (d) are the 3D COP trajectories including pressure and position information. (b) and (e) are the rectified 2D position COP trajectories and (c) and (f) the 1D pressure profiles.

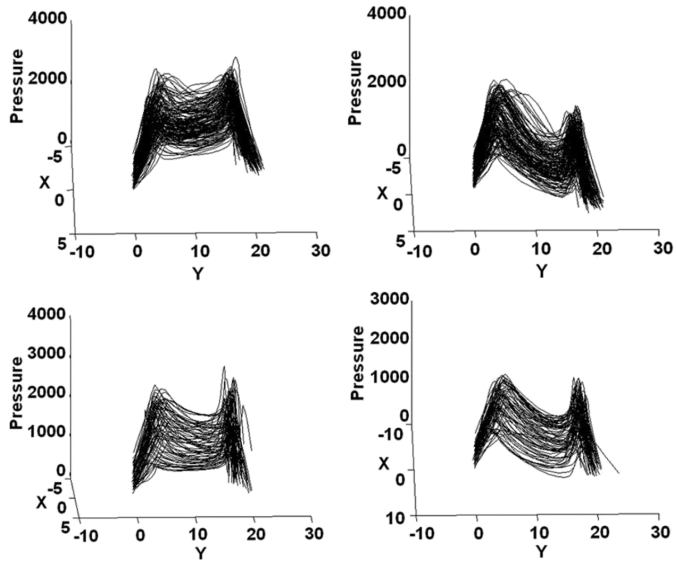

Fig. 3. Samples of the 3D COP trajectories of the left (left panels) and right footsteps from the seventh (first row) and the tenth subjects.

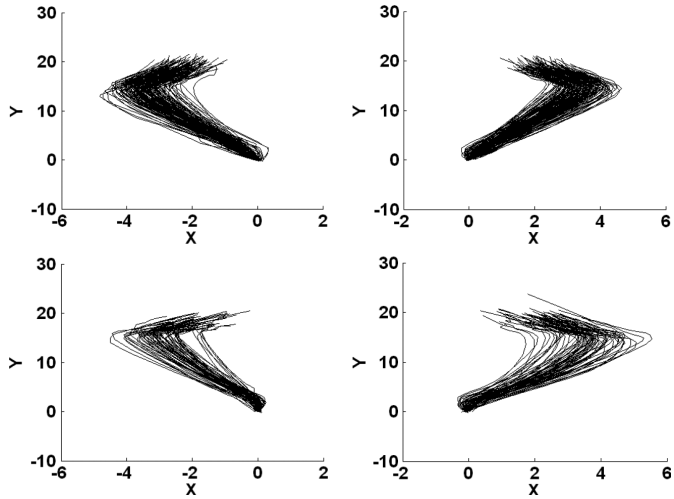

Fig. 4. Samples of the 2D COP trajectories of the left (left panels) and right footsteps from the seventh (first row) and the tenth subjects.

IV. Feature Extraction

It is obvious that the observations we have, i.e., the 3D position-pressure COP trajectories contain all the information used by existing methods, including the footstep-based approaches [8], and the 2D position COP-based approaches [5], [6]. It is expected that by using the comprehensive 3D COP trajectories improved people identification results can be achieved. People identification using gait based on floor pressure is essentially a pattern classification problem, where the dynamic foot pressure distribution of a walking subject is a pattern that need to be recognized and then the subject can be identified. Such a pressure distribution pattern is reflected by the two 3D COP curves during the left and right footsteps. To tackle this classification problem, we need to extract features from the 3D COP trajectories. In our research, we first identify a set of key points along a 3D COP trajectory according to the pressure and position values of the COP and then their pressure reading and/or relative spatial and temporal locations are used in our feature sets. These key points are defined in Table I. Within a footstep, $X_{\max 1}$ corresponds to the toe-off moment of the other foot. $X_{\min}$ appears during full foot contact on the floor. $X_{\max 2}$ takes place when the heel of the other foot is about to strike on the floor. X_t is defined when the absolute value of the x coordinate (orthogonal to walking direction) of COP reach maximum. X_t reflects the

TABLE I
DEFINITION OF KEY POINTS OF A FOOTSTEP

Key point	Definition
X_{max1}	The first dominant local maxima in the pressure trajectory
X_{max2}	The second dominant local maxima in the pressure trajectory
X_{min}	The local minima in the pressure trajectory between Xmax1 and Xmax2
X_t	The turning point in the 2D position COP trajectory
X_{end}	The end of the entire COP trajectory

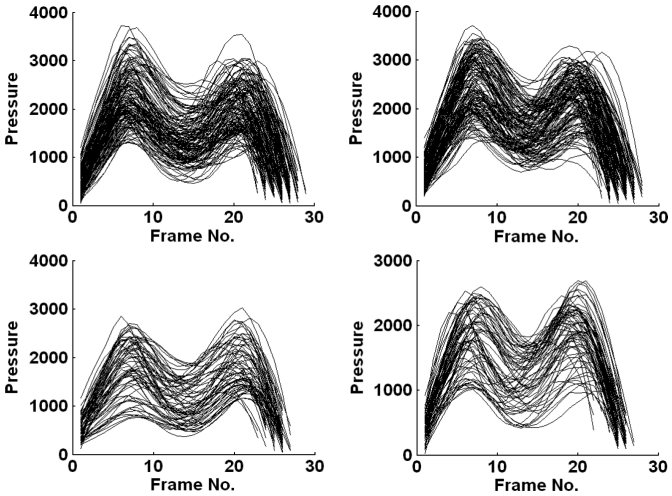

Fig. 5. Samples of the 1D pressure profiles of the left (left panels) and right footsteps from the seventh (first row) and the tenth subjects.

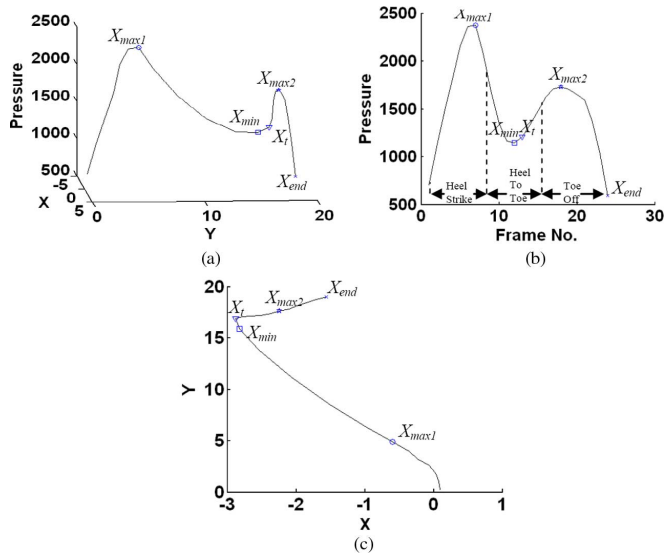

Fig. 6. A typical 3D COP trajectory of (a) left footstep, (b) the related 1D pressure, and (c) 2D position trajectories. The corresponding key points are labeled.

degree of wiggle of the subject during walking. The key points of a typical COP trajectory of a left footstep are shown in Fig. 6. Among these key points, $X_{\max 1}$, $X_{\max 2}$ and $X_{\min}$ are also used by the footstep-based methods, e.g., [7]. In Fig. 6(b), the rough locations of these key points in a pressure profile are presented in terms of gait phases. Note that in our proposed method, there is no need to segment the pressure profile into the gait phase since we only need to detect these key points.

Given a 3D COP trajectory of a footstep, the detection of these key points is straightforward. X_{end} is simply given by the end point of the entire COP per definition. $X_{\max 1}$, $X_{\max 2}$ and $X_{\min}$ are found based on the 1D pressure profile. First, the pressure profile is smoothed by a low-pass filter to suppress noise and then the time derivative of the pressure profile is computed. Then the zero-crossings of the derivative are found as the key point candidates. $X_{\max 1}$ and $X_{\max 2}$ are given by the two key point candidates possessing the largest pressure values while away from each other (e.g., by at least τ frames, $\tau = 8$ in our experiments). $X_{\min}$ is the key point candidate which is between $X_{\max 1}$ and $X_{\max 2}$ and corresponds to the smallest pressure value in this interval. Similarly, X_t is found from the 2D CoP trajectory by treating the 2D COP as a function of Y.

For each key point, the corresponding position, pressure value, and curve length (measured from the start of the COP trajectory), relative frame numbers (counted from the start of the COP) can be used as features. Such key-point-based features from a pair of successive (e.g., right and left) footsteps are used as a feature vector for people identification. In our experiments, we tested different feature combinations and compared their performances. In addition to these features, the sum of the mean pressure of such a pair of successive footsteps is also used as a feature that encodes the body weight of the subjects. Furthermore, stride length is also extracted as part of the feature set.

V. PEOPLE IDENTIFICATION USING FISHER LINEAR DISCRIMINANT

Many existing machine learning algorithms can solve supervised pattern classification problems, including the Bayesian classifiers, the k-nearest neighbors (KNN) method, the support vector machine (SVM) method, and the linear discriminant analysis (LDA) method, just to name a few. An overview of these methods can be found in a standard machine learning textbook, e.g., [3]. In our experiments, we selected the binary version of the LDA, namely, the Fisher linear discriminant (FLD) method as the classifier, due to its simplicity in training and testing. We made use of a MATLAB statistic pattern recognition toolbox [13] for FLD training and testing. In our experiment, we also obtained results using other classifiers such as the KNN and Bayesian classifiers. The comparison between the FLD, KNN and Bayesian classifiers is presented in Section VI-C.

An M-class classification problem can be solved by training M FLD classifiers, one for each class in a one-versus-the-rest framework. For each FLD classifier, training data are split into an in-class sample set which has samples in the corresponding

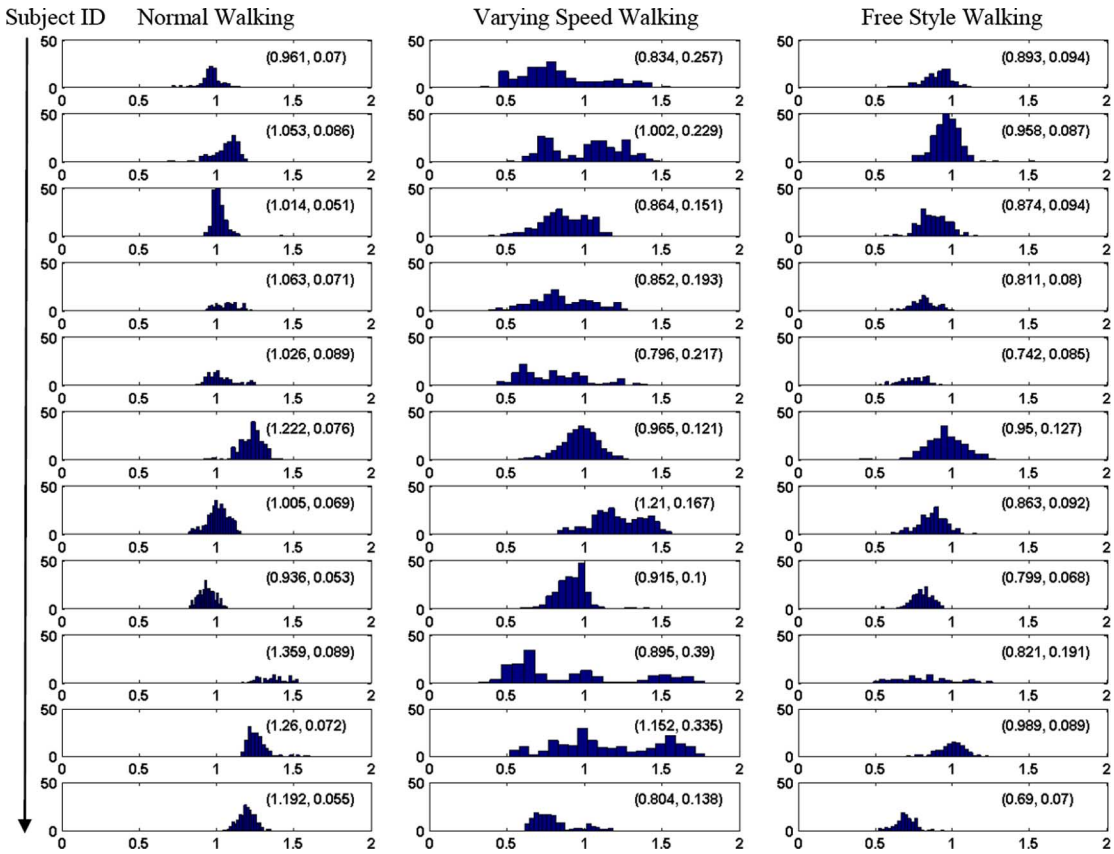

Fig. 7. Histograms of walking speeds of the 11 subjects (rows 1 to 11) for normal walking (left column), varying speed walking (middle column), and varying speed walking. Each subplot is the speed histogram of the corresponding subject and walking style, with the associated mean speed (m/s) and STD given in the upper right corner of the plot.

class and an out-of-class sample set with the remaining training samples of other classes. In the training of an FLD classifier, an optimal linear transformation parameterized by (W, b) needs to be found to maximize the between-class separability and to minimize the within-class variability, thus achieving maximum class discrimination. The parameters (W, b) can be found by solving a generalized eigenvalue problem. Once (W, b) are found, whether a test point x is in the class or not is based on the sign of the discriminant function $q(x)$ given by

$$q(x) = W^T x + b. \tag{3}$$

When $q(x)$ is non-negative, the test point is classified as an in-class data, otherwise, it is not in the class.

VI. Experimental Results and Performance Analysis

A. Data Collection

In our experiments, we collected floor pressure data from 11 subjects, 9 men and 2 women, with an age range of 24–50, and the height range 165–183 cm. For each subject, we collected pressure data for three different walking styles, including normal walking (walking back and forth along a straight path in normal speed), varying speed walking (walking along a straight path but with changing speed), and free walking (walking freely in a 2 m $\times$ 2 m region with changing speed and walking direction and without sharp turns).

In our experiments, the pressure sensing floor ran at a frame rate of 40 Hz. About 4 minute-long pressure data was collected for each subject in each walking style, which included about 9600 frames $(4 \times 60 \times 40)$. After foot recognition and COP tracking using mean-shift, 3D COP trajectories are extracted from pairs of successive footsteps for each subject. In the preprocessing, some data samples were not useable since the key points cannot be reliable extracted from these data samples. Such data samples were then discarded from our experiments. In our experiments, about 25% of collected data were removed for this reason. Finally, in our experiments, 5690 pairs of 3D left and right foot COPs were extracted and used in training and testing, in which 1857 pairs were from normal walking, 2245 pairs from varying speed walking, and 1588 pairs from free style walking.

To illustrate the walking-speed distributions across the three walking styles, we present in Fig. 7 an array of 33 (11 $\times$ 3) speed histograms of the 11 subjects in the three different walking styles. In each speed histogram, the horizontal axis is the walking speed (meters/second) and the vertical axis the number of data samples (footstep pairs) for this subject in this walking style. The mean and standard deviation (STD) of walking speed are also given in the parenthesis at the upper right corner of each subplot. It can be seen that, for most subjects, the speed variations in the varying speed walking dataset is much larger than that in the normal walking dataset, indicated by increased STD and further dispersed spread data samples from the means. In our current MATLAB implementation, to

TABLE II
FOUR FEATURE SETS

Feature set ID	Key points included	Features used for each key point	Other features	Pressure values used?
FS-1	X_{max1}, X_{max2}, X_t, X_{min}, X_{end}	- rectified position, - pressure, - curve length, - relative frame no. normalized by the number of frames of related gait cycle	-stride length - mean pressure of both footsteps	Yes
FS-2	X_{max1}, X_{max2}, X_t, X_{min}, X_{end}	Same as FS-1	- mean pressure of both footsteps	Yes
FS-3	X_{max1}, X_{max2}, X_t, X_{min}, X_{end}	- rectified position, - curve length, - relative frame no. normalized by the number of frames of related gait cycle	-stride length	No
FS-4	X_{max1}, X_{max2}, X_t, X_{min}, X_{end}	Same as FS-3		No

extract features from pressure data of a pair of footsteps (about 50 frames long), it takes about 7.79 s (0.16 s/frame) to track pressure cluster centers, about 0.47 s (9.8 ms/frame) to recognize left and right feet and to form the 3D COP trajectory, and 73 ms to find the key points. The major (93.5%) computational cost in feature extraction is due pressure center clustering and tracking using mean-shift.

B. Feature Selection

In Section III, a number of features are introduced for people identification. Some of the features are related to the key points such as the locations, pressure values, curve lengths, and frame number of the key points, and some of them contain summarizing features of the subject's gait, such as the stride length. In our experiments, we tested different feature sets and compared their performance. Beside the final people recognition results, there is an important aspect we looked into when different feature sets were formed and compared. That is to what extent the feature set is invariant to walking speed. It is ideal to have a people ID system that can recognize a subject across changing walking speed. Therefore, it is important to use feature sets that are invariant to walking speed as much as possible. In addition, we also want to examine how important the pressure information is in people identification. Our hypothesis is that pressure features are more invariant to speed than other features, such as the stride length.

In our experiment, four different set of features shown in Table II were formed and compared. The four feature sets share some common features associated with all five key points defined in Table II, including the rectified position, curve length, and relative frame number normalized by the number of frames of related gait cycle. It is noticeable that this common feature set is independent of both pressure information and possibly, walking speed. Feature set 4 (FS-4) actually contains only these common features. Therefore, FS-4 does not include any pressure or stride length information and possibly it is invariant to walking speed to a large extent. Feature set 3 (FS-3) is augmented based on FS-4 by adding the stride length as an addition feature. Therefore FS-3 is also pressure independent. Stride length can be affected by the walking speed, although walking speed is mainly dominated by the stride cadence. For this reason, FS-3 is not as good as FS-4 in terms of speed-invariance. Feature set 1 (FS-1) is essentially FS-3 plus pressure information, such as the pressure readings at the five key points and the mean pressure of both footsteps. Likewise, feature set 2 (FS-2) is FS-4 plus the same set of pressure features. These four features were derived based on the feature sets used in our previous work [16]. One of the key difference is that cadence is not included in the current feature set to improve speed-invariance. In addition, in [16], FS-2 includes both the stride length and the mean pressure features. While in this paper, FS-2 does not include stride length as a feature.

To examine the speed-invariant properties of these features, for each feature we compute a distance measure based on the Kullback–Leibler divergence (KLD) [22] between the distributions of this feature in different walking styles. To be specific, let X be the feature under examination, and $f_1(x)$, $f_2(x)$, and $f_3(x)$ are the empirical probability density functions of X for the three different walking styles. We define the speed-dependence measure (SDM) for feature X as follows:

$$\mathrm{SDM}_X = \frac{1}{3}\left(D(f_1, f_2) + D(f_2, f_3) + D(f_1, f_3)\right) \quad (4)$$

where $D(f, g)$ is the symmetrical KLD between the two distributions f and g, defined as follows:

$$D(f,g) = \frac{1}{2}\left(\int_{-\infty}^{\infty} f(x)\log\frac{f(x)}{g(x)}dx + \int_{-\infty}^{\infty} g(x)\log\frac{g(x)}{f(x)}dx\right).$$

When both f and g are normal distributions, i.e., $f(x) = N(\mu_1, \sigma_1^2)$ and $g(x) = N(\mu_2, \sigma_2^2)$, $D(f, g)$ can be evaluated as the following:

$$D(f,g) = \frac{1}{4}\left(\frac{\sigma_1^2 + (\mu_1 - \mu_2)^2}{\sigma_2^2} + \frac{\sigma_2^2 + (\mu_1 - \mu_2)^2}{\sigma_1^2} - 2\right).$$

If a feature exhibits a large SDM value, it indicates that this feature is less invariant to speed changes than another feature with a smaller SDM value.

In our experiment, we evaluated such speed-dependence measure for all the features in Table II. We assume for each feature, its distribution for one subject and one walking style follows a

TABLE III
SPEED-DEPENDENCE MEASURE OF THE KEY POINT FEATURES

Key Point	X Position	Y Position	Pressure	Curve Length	Relative Frame Number
Left Xmax1	*0.2487*	*0.9634*	*0.3633*	*0.2643*	*0.7545*
Left Xmin	*0.6538*	*0.8563*	*0.3858*	*0.4958*	*0.3887*
Left Xmax2	*1.6761*	*1.8785*	*0.4711*	*0.8819*	*0.1792*
Left Xt	*0.4978*	*1.6583*	*0.3714*	*0.3090*	*0.7647*
Left Xend	*0.6097*	*2.4165*	*0.15*	*0.3004*	*0.3102*
Right Xmax1	*0.1909*	*0.4416*	*0.4535*	*0.1742*	*0.7384*
Right Xmin	*0.9022*	*0.7332*	*0.3719*	*0.7251*	*0.5899*
Right Xmax2	*1.5895*	*1.6578*	*0.3847*	*1.0321*	*0.1655*
Right Xt	*0.3189*	*1.4099*	*0.4005*	*0.1985*	*0.8145*
Right Xend	*0.7778*	*2.4922*	*0.1814*	*0.4806*	*0.2138*

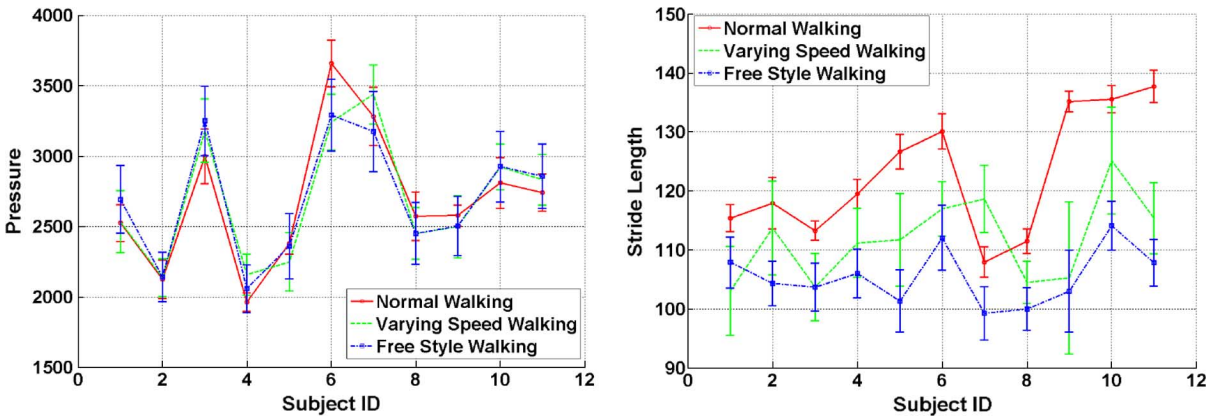

Fig. 8. Mean and STD values of the mean pressure (left panel, in dpv) and stride length (right panel, in cm) features of the 11 subjects in the three different walking styles. At each point, the error bar sits at the mean value with the height equal to the STD. It can be seen that the mean pressure features presents a much more speed invariance property than the stride length feature.

Gaussian distribution. Using (4), for each feature we first evaluated the SDMs for all the subjects separately and then their average over all the subjects was taken as the overall SDM for this feature. The final SDM results computed in this way actually match our hypothesis that pressure features are more speed-invariant than other features, such as the stride length. The SDM value of the stride length feature is 4.1219, which is the largest among all the features. The mean pressure feature over two footsteps has a SDM of 0.4291. The SDMs of the key point features are given in Table III. It can be seen that the pressure features consistently exhibit low SDM values over all key points. To take a closer look at the speed-invariance properties of the stride length and mean pressure features, we further examined them for each individual subject. Fig. 8 shows the mean and STD values of the mean pressure (left) and stride length features of the 11 subjects in the three different walking styles. At each point, the error bar sits at the mean value with the height equal to the STD. Consistent to what the SDM values indicate, it can also be seen from Fig. 8 that the mean pressure feature presents a much more speed invariance property than the stride length feature. Therefore, it is expected that in the presence of large speed variations, FS-2 using pressure features will perform better than FS-3, which uses the stride length feature. This has been verified by the people identification results presented in the next section.

C. Cross Validation and Performance Analysis

To validate the performance of different feature sets and obtain an overall picture of the proposed approach, we ran cross-validation over the entire data set. One hundred runs were taken. For each run, 70% of total COP pairs were drawn randomly from the entire data set as training data. The remaining samples were then used as testing data. In each run, using the same training and testing sets, the results obtained using the four feature sets were compared. The recognition rate (RR) and the false alarm rate (FAR) are used to evaluate the performance of the proposed people identification method. The RR is defined as the ratio of the number of correct recognitions (NCR) and number of total in-class data (NTI). The FAR is the ratio between the number of false alarms (NFA) and the number of total outclass data (NTO)

$$\mathrm{RR} = \frac{\mathrm{NCR}}{\mathrm{NTI}} \times 100\%, \quad \mathrm{FAR} = \frac{\mathrm{NFA}}{\mathrm{NTO}} \times 100\%. \qquad (5)$$

Fig. 9 shows the resulting RR (left panel) and FAR over 100 trials using the four feature sets. The results for each trial are the average RR and FAR of the 11 subjects. It can be seen that FS-1 has the best performance with the highest RR (92.3% in average) and lowest FAR (6.79% in average), while FS-4 has the worst performance. This result indicates that both the pressure features and stride length are contributing features to people recognition. It is important to include both stride length and

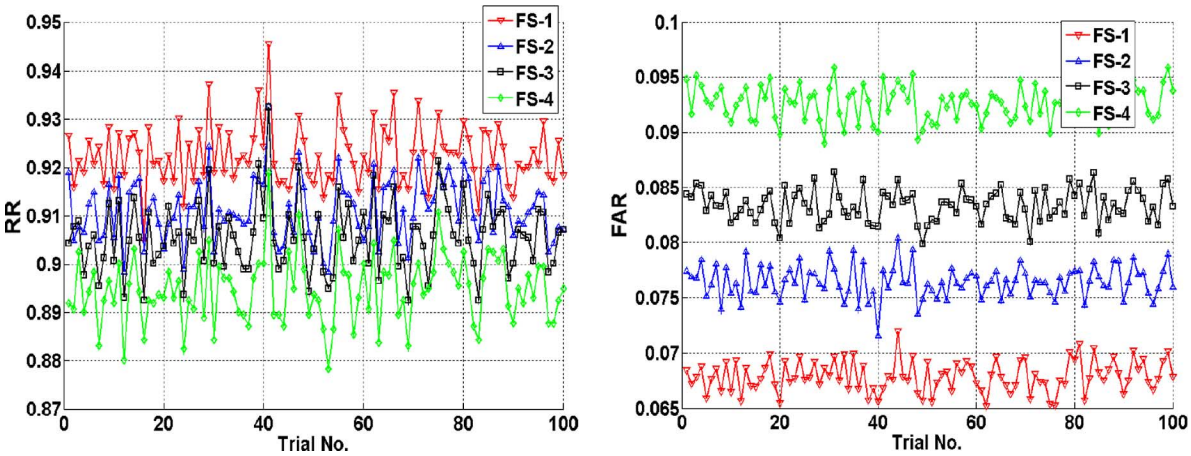

Fig. 9. The RR (left) and FAR of 100 trials using the four feature sets.

TABLE IV
AVERAGE RECOGNITION RESULTS OF FS-1 AND FS-2 OVER 100 TRIALS

Subject ID#	Recognition					False Alarm				
	NTI	**FS-1**		**FS-2**		NTO	**FS-1**		**FS-2**	
		NCR	*RR* %	NCR	*RR* %		NFA	*FAR* %	NFA	*FAR* %
1	129	117	*90.3*	115	*89.5*	1574	81	*5.1*	83	*5.3*
2	190	178	*93.7*	178	*93.5*	1513	93	*6.1*	93	*6.1*
3	183	165	*89.9*	165	*89.9*	1520	128	*8.4*	128	*8.4*
4	112	101	*90.5*	101	*90.4*	1591	123	*7.7*	125	*7.9*
5	101	93	*91.9*	91	*90.3*	1602	125	*7.8*	137	*8.6*
6	197	186	*94.2*	186	*94.3*	1506	68	*4.5*	70	*4.6*
7	224	217	*96.8*	211	*94*	1479	77	*5.2*	129	*8.7*
8	182	171	*93.9*	171	*93.7*	1521	85	*5.6*	86	*5.7*
9	90	80	*89.2*	79	*88.3*	1613	127	*7.9*	142	*8.8*
10	151	122	*80.8*	113	*75.1*	1552	224	*14.4*	284	*18.3*
11	144	142	*98.6*	142	*98.6*	1559	26	*1.7*	26	*1.7*
Overall	**1703**	**1572**	***92.31***	**1552**	***91.13***	**17030**	**1157**	***6.79***	**1303**	***7.65***

TABLE V
AVERAGE RECOGNITION RESULTS OF FS-3 AND FS-4 OVER 100 TRIALS

Subject ID#	Recognition					False Alarm				
	NTI	**FS-3**		**FS-4**		NTO	**FS-3**		**FS-4**	
		NCR	*RR* %	NCR	*RR* %		NFA	*FAR* %	NFA	*FAR* %
1	129	116	*89.7*	115	*88.8*	1574	88	*5.6*	94	*6*
2	190	168	*88.2*	168	*88.2*	1513	125	*8.3*	126	*8.3*
3	183	163	*89.1*	163	*89*	1520	156	*10.3*	155	*10.2*
4	112	98	*87.7*	98	*87.6*	1591	144	*9.1*	145	*9.1*
5	101	90	*88.7*	88	*87.1*	1602	154	*9.6*	167	*10.4*
6	197	184	*93.6*	183	*93.1*	1506	92	*6.1*	93	*6.2*
7	224	212	*94.8*	209	*93.1*	1479	126	*8.5*	180	*12.2*
8	182	170	*93.4*	169	*92.9*	1521	98	*6.4*	103	*6.8*
9	90	79	*88*	77	*86*	1613	157	*9.7*	175	*10.8*
10	151	121	*79.8*	113	*74.7*	1552	247	*15.9*	305	*19.7*
11	144	142	*98.5*	142	*98.4*	1559	32	*2.1*	33	*2.1*
Overall	**1703**	**1543**	***90.6***	**1525**	***89.55***	**17030**	**1419**	***8.33***	**1576**	***9.25***

pressure values as part of the feature vector. The average performances of the proposed methods with the four feature sets for each person are presented in Tables IV and V.

To further study the contribution of pressure feature (i.e., FS-2) and stride length (i.e., FS-3) in people recognition, we examined the RR and FAR using different features over three individual datasets. The breakdown results are shown in Fig. 10 and Table VI. Fig. 10 includes RR (left panels) and FAR results using different datasets and feature sets. It can be seen from Table VI that for all walking styles, FS-2 performs consistently better than FS-3. Especially in the cases of varying speed and free style walking, the RR and FAR of FS-2 are noticeably better than those of FS-3. This comparison shows that the pressure feature is more contributory to people identification than the stride length in the cases of varying speed and free style walking.

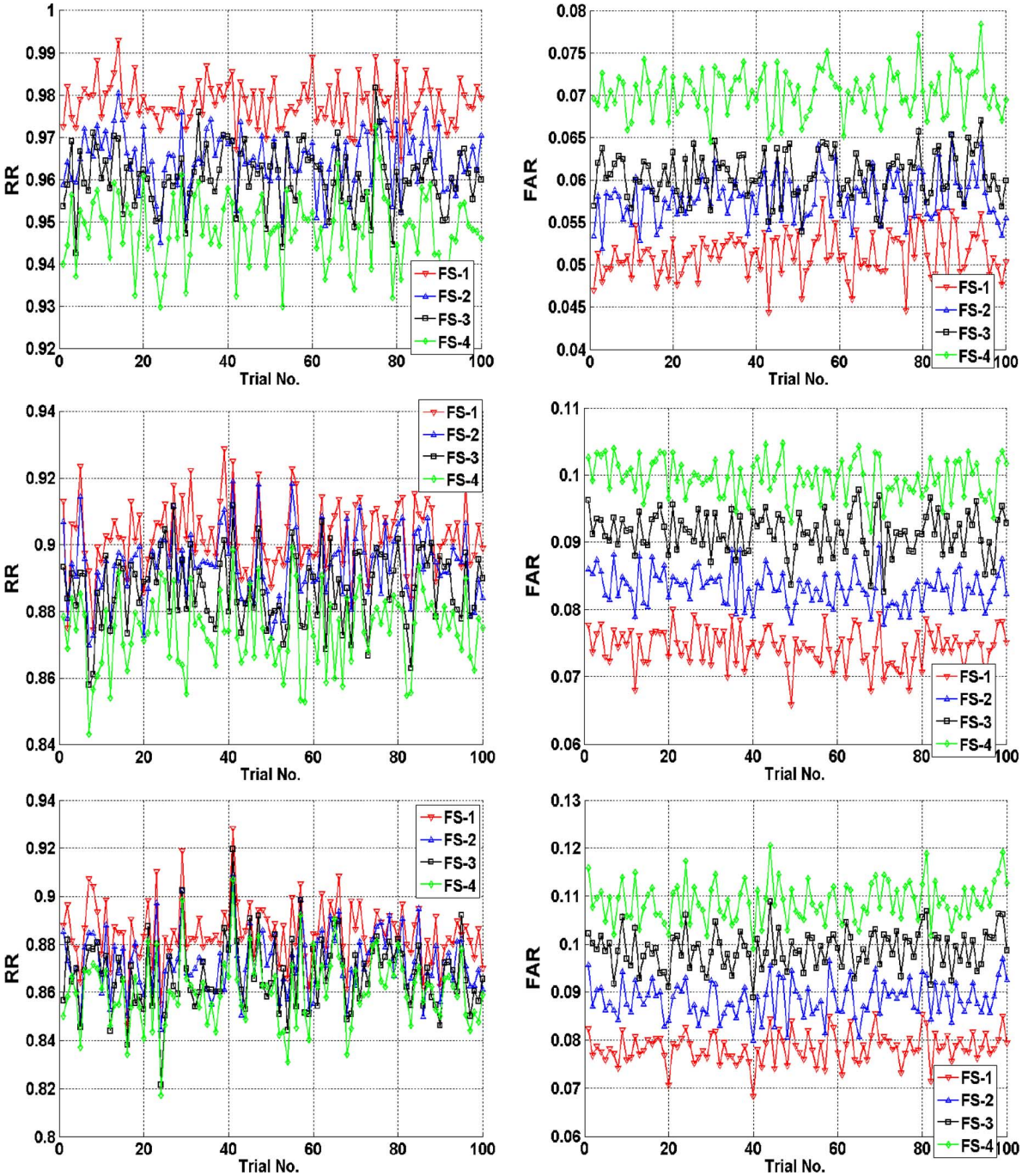

Fig. 10. The RR (left) and FAR of 100 trials using the four feature sets applied to different testing datasets: normal walking (top row), varying speed walking (middle row), and free style walking.

In our experiment, we also used the KNN and Bayesian classifiers for people identification using the same training and testing data as those used by FLD. For these two classifiers, we again used their implementations in the MATLAB statistic pattern recognition toolbox [13]. The corresponding people identification results are shown in Table VII. It can be seen from Table VII that KNN and Bayesian classifiers present similar people identification results. The RR and FAR obtained using the KNN and Bayesian classifiers are both lower that those obtained using FLD. This makes senses since there is a trade-off between high RR and low FAR. We also compared the time consumed by the training and testing processes using different classifiers and the results are given in Table VIII. It is clear that as far as the training is concerned, the KNN and Bayesian are both more computationally efficient than FLD. On the other hand, KLD is much faster than the KNN and Bayesian classifiers in testing. Efficient testing is more important than training for real-time applications.

In addition, we also compared the results of the proposed method to those of the existing people identification methods using floor pressure. The comparison is summarized in Table IX. It can be seen that according to the features used, existing methods can be roughly clustered into methods using only pressure profiles [1], [8]–[10], [17], methods using only

TABLE VI
AVERAGE RECOGNITION RESULTS OF FOUR FEATURES SETS OVER THE THREE INDIVIDUAL DATA SETS

	Normal Walking		Varying Speed Walking		Free Walking	
	RR %	*FAR %*	*RR %*	*FAR %*	*RR %*	*FAR%*
FS-1	97.82	5.11	90.27	7.44	88.48	7.84
FS-2	96.49	5.80	89.40	8.32	87.27	8.86
FS-3	96.06	6.05	88.70	9.15	86.75	9.89
FS-4	94.81	7.04	87.44	9.96	86.11	10.89

TABLE VII
AVERAGE RECOGNITION RESULTS USING THE FLD, KNN AND BAYESIAN CLASSIFIERS FOR DIFFERENT FEATURE SETS

	FS-1		FS-2		FS-3		FS-4	
	RR %	*FAR %*	*RR %*	*FAR %*	*RR %*	*FAR %*	*RR %*	*FAR %*
FLD	92.24	6.79	91.13	7.65	90.57	8.34	89.48	9.26
KNN-3	81.67	1.83	79.91	2.01	78.12	2.19	76.11	2.39
KNN-5	82.11	1.79	80.63	1.94	78.34	2.13	76.49	2.35
KNN-7	82.03	1.80	80.60	1.94	78.02	2.20	76.31	2.37
Bayesian	86.36	1.36	84.42	1.56	81.92	1.81	79.67	2.03

TABLE VIII
AVERAGE TIME (SECONDS) USED BY THE FLD, KNN AND BAYESIAN CLASSIFIERS FOR EACH RUN

	FS-1		FS-2		FS-3		FS-4	
	Training	*Testing*	*Training*	*Testing*	*Training*	*Testing*	*Training*	*Testing*
FLD	0.2221	0.0066	0.2266	0.0058	0.1720	0.0014	0.1570	0.0044
KNN-3	0.0002	10.79	~0	10.59	~0.0001	8.57	0.0003	8.37
KNN-5	~0	10.83	~0	10.63	0.0002	8.61	~0	8.41
KNN-7	0.0002	10.87	~0	10.67	0.0002	8.65	~0	8.45
Bayesian	0.0179	0.0662	0.0162	0.0685	0.0130	0.0521	0.0121	0.0489

2D positional COP trajectories [5], [6], and methods based on explicit gait features such as stride length, cadence [7], [11], [12], [18]. In general, the method only using 2D COP performed the worst among all the methods. Excellent people recognition results have been reported using the pressure profile [8] and gait features [11], [12]. The features used in our proposed method explore the 3D COP trajectories which contains both the pressure profiles and the 2D positional trajectories. In addition, the stride length is also used in the proposed method. Therefore, the proposed method makes use of a nearly comprehensive feature sets which include the key features of the existing methods. This is made possible by using a high-resolution pressure sensing floor and robust pressure clustering and tracking algorithm using mean-shift. As the result, the performance of the proposed approach is superior or comparable to nearly all the existing methods.

Some existing results reported previously appear to be better than ours. For example, the people recognition rate reported in [8] is 93% from a testing population of 15 people. Based on testing populations of 10 subjects, the reported recognition rates in [11] and [12] are 96.2% and 92.8%, respectively. However, due to the use of time features in these methods in [8], [11], [12], these people identification methods are not invariant to the walking speed. To the contrast, our proposed methods are either partially (FS-1, FS-3) or completely (FS-2, FS-4) invariant to walking speeds. In addition, none of the results of the existing methods, except those in [17] and [18], was based on cross-validation as what we have done in our research. Hence, it is not clear whether the reported non-cross-validated recognition results of the existing methods were based on results of a number of trials or just one trial. The performance of an algorithm can vary by different selection of training and testing data set. In the first column to the right of Table IX, we have included the ranges and STDs of the RRs and FARs of our proposed methods using different feature sets. It can be seen that the peak RR for FS-1 is 94.5%.

Multiple footsteps have been exploited to improve the recognition results. For example, in [11] and [12], five consecutive footsteps were used and in [21], features were extracted from two or four footsteps. In [17], people recognition performances of using different number of footsteps are reported and compared. It is clear from these existing results that using multiple footsteps can definitely greatly improve the people recognition rate. On the other hand, the requirement of multiple footsteps for recognition is somewhat limiting the capacity of the people identification system. In our proposed framework, only two footsteps are used for people identification. Moreover, compared to [11], [12], [17], and [21], one of the strengths of the proposed approach is that it has shown good performance using data collected in more realistic situations, for example, with varying speed and free style walking.

Recently, Suutala and Röning present in [17] a systematic performance analysis and comparison for pressure sensing-based people recognition in terms of different pressure and temporal feature sets, classifiers, and number of footsteps, and methods for fusing results from multiple footsteps. For example, performances of KNN, SVM, multilayer perceptron (MLP), learning vector quantization (LVQ), and radial basis function (RBF) are compared. Different from [11] and [12] in the way that multiple footsteps are used, instead of forming

TABLE IX
PERFORMANCE COMPARISON OF METHODS FOR PEOPLE IDENTIFICATION USING FLOOR PRESSURE

Method	Floor sensor	Major features	Classifiers	# of sub.	RR (%)	FAR (%)	Cross Validated?
Addlesee et al., 1997, [1]	Load-cells	Pressure profile over a footstep	HMM	15	<50	N/A	No
Jung et al., 2003, [5]	Pressure mats	2D trajectories of COP	HMM	8	64	5.8	No
Pirttikangas et al., 2003, [9]	Pressure floor	Pressure profile over the entire floor during walking	HMM	3	76.9	11.6	No
Pirttikangas et al., 2003, [10]	Same as [9]	Same as the above [9]	LVQ	11	<78	N/A	No
Jung et al., 2004, [6]	Pressure mats	2D positional trajectories of COP	HMM-NN	11	79.6	2.05	No
Middleton et al., 2005, [7]	Force sensitive resistor (FSR) mats	Stride length, stride cadence, heel-to-toe ratio	N/A	15	80	N/A	No
Yun et al., 2003, [12]	Floor w/ on/off switch sensors,	Compensated foot centers over **5** consecutive footsteps	MLP	10	92.8	N/A	No
Orr et al., 2000, [8]	Load-cells	Key points from pressure profile	KNN	15	93	N/A	No
Yoon et al., 2005, [11]	Floor w/ on/off switch sensors,	Compensated foot centers and heel-strike and toe-off time over **5** consecutive footsteps	MLP	10	96.2	N/A	No
Yoon et al., 2008, [21]	Floor w/ on/off switch sensors	The left footprint pattern and the array of sampled transitional footprints over different combinations of 2 or 4 footsteps	MLP	10	92 (the case using 4 footsteps)	N/A	No
Suutala and Röning, 2008, [17]	Pressure floor, same as [9]	Pressure and time features extracted from pressure profile over a footstep	MLP	10	63.3 (single footstep)	N/A	Yes RR STD: 2.6
			SVM		81.9 (two footsteps)	N/A	Yes RR STD: 3.4
					91.7 (five footsteps)		Yes RR STD:2.5
Suutala et al., 2008, [18]	Floor w/ on/off switch sensors,	**Single Footstep**: length, width, duration, number of pixels in the binary map, (min, max, mean, std) from the gray-level duration map, **Between footsteps**: stride length, stride cadence,	GP	9	64 (single footstep)	N/A	Yes RR STD: 3.3
					84(sequence of 5-7 footsteps)	N/A	Yes RR STD: 6.7
Proposed- FS-1	**FSR mats**	**See Table 2**	**FLD**	**11**	**92.31**	**6.79**	**Yes RR: 90.49-94.54, STD: 0.63**
							FAR:6.52-7.19 STD: 0.14
Proposed- FS-2	**FSR mats**	**See Table 2**	**FLD**	**11**	**91.13**	**7.65**	**Yes RR: 89.84-93.25, STD: 0.64 FAR:7.16-8.04 STD: 0.15**
Proposed- FS-3	**FSR mats**	**See Table 2**	**FLD**	**11**	**90.6**	**8.33**	**Yes RR: 89.25-93.25 STD: 0.72 FAR: 7.99-8.64 STD: 0.15**
Proposed- FS-4	**FSR mats**	**See Table 2**	**FLD**	**11**	**89.55**	**9.25**	**Yes RR: 87.84-91.9 STD: 0.69 FAR: 8.9-9.59 STD: 0.16**

a concatenated feature vector from multiple footsteps, in [17] the posterior probability of person given the features are first obtained for each individual step. The final recognition based on multiple footsteps is cast into an information fusion problem at the level of the posterior probability using different rules of combining classifiers [19]. Results reported in [17] are cross-validated using ten trials. The key features used in [17] are extracted from the pressure profiles, without 2D COP information. The best results for one footstep and two and five footsteps reported in [17] are included in Table IX. It can be seen that these results using one and two footsteps are inferior to what we have obtained. Suutala *et al.* have also used the Gaussian processes method for people recognition using a low-resolution binary on/off switch floor [18]. Both single and multiple footsteps are used for recognition. In [18], the reported results are also cross-validated using ten trials. As shown in Table IX, our results are much better than that in [18].

Compared to existing methods, another advantage of our proposed method is that it uses Fisher linear discriminant, which is a much more computationally efficient method than those used by existing methods such as Gaussian processes, hidden Markov models and neural networks. This makes the training and testing of the proposed method very fast. Using MATLAB, it takes only about 103 s to run the 100 trials with each trial including the training and testing of the four feature sets for 11 subjects. In average, it takes 227.1 ms to run training and 3.8 ms to run testing for the 11 subjects with one feature set using 3983 training and 1707 testing samples. We attribute this advantage to the use of 3D COP trajectories in the pressure and position spaces and corresponding derived feature sets.

VII. Conclusion and Future Work

A robust people identification approach using gait based on floor pressure is presented in this paper. Promising people identification results have been obtained by using features extracted from the 3D COP trajectories in the pressure and position spaces. The proposed approach makes use of simple linear classifiers for fast real-time recognition from extracted features. This indicates that the features used in our approach from different people are mostly linearly separable. In the selection of the feature set, we have also considered the issue of walking-speed invariance by normalizing the time stamps of the key points by the length of the corresponding gait cycle. We have shown that the pressure features have good speed-invariance properties, much better than the stride length feature. The proposed approach has led to better or comparable people recognition results compared to existing methods for people identification using floor pressure.

One of the limitations of the reported results in this paper is that the current experiments were done with shoes off. In our future work, we will evaluate and fine-tune our proposed method to see how it can recognize people in shod scenarios. Furthermore, we will evaluate the system performance by using more foot steps to better compare the proposed approach to that in [11]. In addition, the proposed people identification system is intended for recognizing one user at a time. The proposed system can be extended for concurrent identification of multiple people if they walk in nonoverlapping individual subsections of the pressure sensing floor. On the other hand, to simultaneous recognize multiple people walking on the entire floor, possibly in intersecting trajectories, requires further research in our future work. The key challenge to be addressed is reliable tracking of multiple people from floor pressure data.

Pressure sensors have been integrated with other sensors including tile angle sensor, gyroscope, bend sensor, and accelerometer for people identification using gait [4]. Excellent people identification results have been reported in [4] based on a testing population of nine subjects. The approach proposed in [4] makes use of pressure sensors of low spatial resolution. Another research direction we will pursue in the future is to integrate the high-resolution pressure sensing floor with other sensors such as those used in [4] to further improve people identification using gait, e.g., by increasing the size of testing population that the system can reliably recognize.

Acknowledgment

The authors are thankful to the reviewers for their insightful comments and suggestions. This material is extended based on the following article of the authors, with kind permission of Springer Science + Business Media: G. Qian, J. Zhang, and A. Kidané, "People Identification Using Gait via Floor Pressure Sensing and Analysis," in *Proceedings of the IEEE European Conference on Smart Sensing and Context*, LNCS 5279, pp 83–98, Springer-Verlag GmbH, Berlin, Heidelberg, 2008.

References

[1] M. Addlesee, A. Jones, F. Livesey, and F. Samaria, "The ORL active floor," *IEEE Pers. Commun.*, pp. 35–41, Oct. 1997.

[2] Y. Cheng, "Mean shift, mode seeking and clustering," *IEEE Trans. Pattern Analy. Mach. Intell.*, vol. 17, no. 8, pp. 790–799, 1995.

[3] R. O. Duda, P. E. Hart, and D. G. Stork, *Pattern Classification*, 2nd ed. New York: Wiley, 2000.

[4] B. Huang, M. Chen, P. Huang, and Y. Xu, "Gait modeling for human identification," in *Proc. IEEE Int. Conf. Robot. Autom.*, 2007, pp. 4833–4838.

[5] J. Jung, Z. Bien, S. Lee, and T. Sato, "Dynamic-footprint based person identification using mat-type pressure sensor," in *Proc. Int. Conf. IEEE Eng. Med. Biol. Soc.*, 2003, vol. 3, pp. 2937–2940.

[6] J. Jung, T. Sato, and Z. Bien, "Dynamic footprint-based person recognition method using a hidden Markov model and a neural network," *Int. J. Intell. Syst.*, vol. 19, no. 11, pp. 1127–1141, 2004.

[7] L. Middleton, A. A. Buss, A. Bazin, and M. S. Nixon, "A floor sensor system for gait recognition," in *Proc. IEEE Workshop on Autom. Identification Adv. Technol.*, 2005, pp. 171–176.

[8] R. J. Orr and G. D. Abowd, "The smart floor: A mechanism for natural user identification and tracking," in *Proc. Conf. Human Factors in Comput. Syst.*, 2000, pp. 275–276.

[9] S. Pirttikangas, J. Suutala, J. Riekki, and J. Röning, "Footstep identification from pressure signals using hidden Markov models," in *Finnish Signal Process. Symp.*, 2003, pp. 124–128.

[10] S. Pirttikangas, J. Suutala, J. Riekki, and J. Röning, "Learning vector quantization in footstep identification," in *Proc. IASTED Int. Conf. Arti. Intell. Appl.*, 2003, pp. 413–417.

[11] J. Yoon, J. Ryu, and W. Woo, "User identification using user's walking pattern over the ubiFloorII," in *Proc. Int. Conf. Comput. Intell. Security*, 2005, vol. 3801, pp. 949–956.

[12] J. Yun, S. Lee, W. Woo, and J. Ryu, "The user identification system using walking pattern over the ubiFloor," in *Proc. Int. Conf. Control, Autom. Syst.*, 2003, pp. 1046–1050.

[13] V. Franc and V. Hlavac, Statistical pattern recognition toolbox for Matlab user's guide, Center for Machine Perception, K13133 FEE Czech Technical Univ., Res. Rep. CTU-CMP-2004-08, 2004.

[14] S. Rangarajan, A. Kidane, G. Qian, and S. Rajko, "The design of a pressure sensing floor for movement-based human computer interaction," in *Proc. Eur. Conf. Smart Sensing and Context*, 2007, vol. 4793, LNCS, pp. 46–61.

[15] S. Rangarajan, A. Kidane, G. Qian, and S. Rajko, "Design optimization of pressure sensing floor for multimodal human computer interaction," in *Advances in Human Computer Interaction*. Vienna, Austria: I-Tech Education and Publishing, 2008.

[16] G. Qian, J. Zhang, and A. Kidane, "People identification using Gait via floor pressure sensing and analysis," in *Proc. 3rd Eur. Conf. Smart Sensing and Context (EuroSSC)*, Zürich, Switzerland, Oct. 29–31, 2008, vol. 5279, LNCS, pp. 83–98, \\dma.asu.edu\wwwroot\faculty\qian\Publications\PressureSensingFloor_MHCI_FINAL.pdf.

[17] J. Suutala and J. Röning, "Methods for person identification on a pressure-sensitive floor: Experiments with multiple classifiers and reject option," *Inf. Fusion*, vol. 9, no. 1, pp. 21–40, Jan. 2008.

[18] J. Suutala, K. Fujinami, and J. Röning, "Gaussian process person identifier based on simple floor sensors," in *Proc. 3rd Eur. Conf. Smart Sensing and Context (EuroSSC_2008)*, Zurich, Switzerland, Oct. 2008, pp. 55–68.

[19] J. Kittler, M. Hatef, R. P. W. Duin, and J. Matas, "On combining classifiers," *IEEE Trans. Pattern Analy. Mach. Intell.*, vol. 20, no. 3, pp. 226–239, 1998.

[20] D. Comaniciu and P. Meer, "Mean shift: A robust approach toward feature space analysis," *IEEE Trans. Pattern Analy. Mach. Intell.*, vol. 24, no. 5, pp. 603–619, 2002.

[21] J. Yun, G. Abowd, J. Ryu, and W. Woo, "User identification with user's stepping pattern over the ubiFloorII," *Int. J. Pattern Recogn. Artif. Intell. (IJPRAI)*, vol. 22, no. 3, pp. 497–514, 2008.

[22] S. Kullback, *Information Theory and Statistics*. New York: Wiley, 1959.

[23] I. Rosenberg and K. Perlin, "The UnMousePad: An interpolating multi-touch force-sensing input pad," in *Proc. ACM SIGGRAPH* , H. Hoppe, Ed., Orleans, LA, Aug. 3–7, 2009.

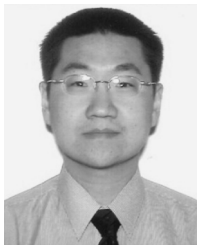

Gang Qian (S'00–M'01) received the Ph.D. degree in electrical engineering from the University of Maryland, College Park, in 2002. He received the Guo-Moruo Gold Medal when he graduated from the University of Science and Technology of China, Hefei, in 1995, with a B.E. degree in electrical engineering.

He is currently an Assistant Professor with the School of Arts, Media and Engineering and the School of Electrical, Computer and Energy Engineering, Arizona State University. His main research interests include computer vision and pattern analysis, sensor fusion and information integration, human-centered interactive systems, machine learning for computer vision, and multimodal sensing and analysis of human activities for embodied learning and movement rehabilitation.

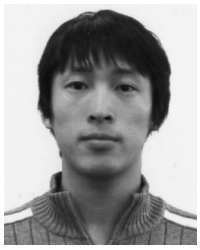

Jiqing Zhang was born in Jiamusi, China, in 1984. He received the M.S. degree in electrical engineering from Arizona State University, Tempe, in 2009.

From August 2007 to May 2009, he was a Research Assistant at the School of Arts, Media and Engineering, focusing on human movement sensing and analysis via floor pressure data using computer vision, pattern classification and image processing technology.

Assegid Kidané (M'00) is an Experiential Media Engineer at the School of Arts, Media and Engineering (AME), Arizona State University, Tempe. In this capacity, he collaborates with a diverse group of faculty, students, and staff from AME and a multitude of other disciplines leading the physical realization of smart devices. His research interests are multimodal sensing and actuation, embedded control and motion analysis.